Invited Paper

AlGaSb/GaSb Metal-Semiconductor-Metal Detectors Grown on InP substrates (Invited Paper)

Y. Wang, M. C. Teich, and W. I. Wang

Department of Electrical Engineering, Columbia University

New York, NY 10027

ABSTRACT

$Al_{0.5}Ga_{0.5}Sb$/GaSb metal-semiconductor-metal (MSM) detectors have been prepared on semi-insulating InP substrates. The molecular beam epitaxially grown samples on differently oriented substrates exhibit different types of conductivity. The Schottky barrier height between Al and $Al_{0.5}Ga_{0.5}Sb$ grown on (311)B oriented substrates is 0.6 eV, while the Al contacts on (100) sample exhibit ohmic behavior. The results show that the Sb-deficiency related p-type native defect density is significantly reduced in the samples grown on (311)B oriented substrates. The 3-dB device response bandwidth is about 1 GHz at room temperature and beyond 10 GHz at 77 K.

The metal-semiconductor-metal (MSM) photodetectors offer the fundamental advantages of extremely low device capacitance and compatibility with MESFETs technology. These advantages are favorable for optical fiber receivers in high speed and low noise operation. Due to their unique planar structure, the capacitance of MSM photodetectors is very low. It has been shown that an integrated photoreceiver

 0-8194-1013-6/92/$4.00

using a MSM photodetector, rather than a p-i-n photodiode, is inherently more sensitive at high communication data rates, despite the reduced responsivity caused by the metal finger shadowing.[1]

The material most commonly used for photoabsorption layer for 1.3-1.6 μm wavelength is $In_{0.53}Ga_{0.47}As$, which is lattice-matched to the InP substrate. However, the Schottky barrier height on n-type InGaAs is too low (0.2 eV) to accomplish an InGaAs MSM photodetector with a low dark current,[2] which is necessary for a low-noise photoelectronic receiver. Since InGaAs does not form a satisfactory Schottky contact, a thin wide bandgap InAlAs[3] or InP[4] layer has been introduced between the InGaAs and the metal contacts. The devices with this kind of barrier-enhancement layer have shown improved performance with a very low dark current.[3,4] However, in this kind of structure, large band offsets exist both in conduction band and valence band at the InGaAs-InAlAs or InGaAs-InP heterointerface. These band discontinuities will give rise to significant charge storage problems, especially hole storage due to the fact that the mobility of holes is much lower than electrons. These devices only show large bandwidth (>5 GHz) when they are biased at large voltages (10 V). These large bias voltages are required to enhance the velocity of holes as well as their emission across the barrier, which is a result of the band discontinuities at the heterointerface. Thus optimum performance of MSM photodetectors requires a compromise between the low dark current and the small carrier storage, and hence a high hole mobility and less hole storage at the heterointerface are crucial for the high speed operation of MSM photodetectors.

Besides InGaAs, GaSb is another attractive semiconductor material for 1.3-1.6 μm photodetectors. GaSb is a direct bandgap semiconductor with a bandgap of 0.725

eV and a hole mobility as high as about 700 $cm^2.V^{-1}.s^{-1}$ at 300 K for the undoped material which usually shows 10^{17} cm^{-3} p-type. GaSb, like InGaAs, has a high absorption coefficient for 1.3 and 1.5 μm radiation. The Fermi level at a $In_{0.53}Ga_{0.47}As$ surface pins close to the conduction band and at the GaSb surface pins close to valence band.[5] At room temperature, the Schottky barrier height of Au on n-type GaSb was measured about 0.6 eV by Mead.[5] This large Schottky barrier height is favorable for low dark current MSM photodetectors. With an AlGaSb barrier-enhancement layer the dark current would be further reduced while the lower effective hole mass in the alloy systems employing GaSb would continue to result in improved hole collection properties. Therefore, it is expected that the MSM detectors with AlGaSb/GaSb heterostructure will have better performance than InGaAs/InAlAs or InGaAs/InP MSM detectors. This expected better performance and process compatibility with GaSb-based p-channel FET and InAs n-channel FET technologies make GaSb/AlGaSb a very attractive material system for MSM photodetectors.[6-8]

The major difficulty for GaSb MSM detector fabrication is to obtain lightly n-doped epitaxial layer, which is required for a low dark current MSM detector with a low device capacitance. As mentioned above, the undoped GaSb epilayer shows p-type conductivity. The typical doping level for a MBE grown GaSb epilayer on (100) substrate is 10^{17} cm^{-3} p-type. This p-type conductivity is owing to the Ga antisite defects in GaSb, which is a result of Sb deficiency during GaSb growth, and not residual impurities.[9] These defects have to be reduced in order to obtain lightly n-doped GaSb because it is very difficult to compensate a 10^{17} cm^{-3} p-type material into a 10^{15} cm^{-3} or $1x10^{16}$ cm^{-3} n-type material reproducibly. Therefore, in order to improve the quality of MBE grown GaSb and obtain lightly n-doped GaSb epilayer, it is

necessary to produce a more Sb-rich growth environment. As demonstrated in our work, the Sb rich growth environment can be realized by growing GaSb on (311)B oriented substrates rather than (100) oriented substrates.

Among all crystal orientations, the most Sb-rich surface is the (111)B surface. On the (111)B face, as shown in Fig. 1, the surface is Sb rich with each Sb atom having three backbonds and one surface dangling bond. In comparison, the (100) face has both Ga and Sb sites with each site having two backbonds. Therefore, the (111)B surface, which has a higher Sb sticking coefficient than the (100) face, will yield a larger Sb surface concentration for a given impinging Sb flux value. However, growth on (111)B oriented substrates often results in rough morphology due to the high sticking coefficient and low mobility of Sb at (111)B surface. On the (100) and its vicinal surfaces, it is well established that growth proceeds by the step-terrace-kink growth mechanism. Growth of GaSb on these surfaces usually results in good surface morphology but relative higher native defects due to the Sb deficiency. Therefore, it is expected that for GaSb, the optimal growth condition lies somewhere between the (100) and (111)B planes. In general, planes closer to the (111)B will produce lower p-type native defect densities while those closer to the (100) will provide better morphology.

In contrast to (111)B and (100) orientations, the surfaces oriented between (111)B and (100), such as (211)B, (311)B, and (511)B, are composed of both single-dangling bond sites and and double dangling bond sites, making the surface partially (111)B-like and partially (100)-like. In the case of (211)B surface, there are twice as many (111)B-like sites as there are (100)-like sites, Thus, the (111)B-like character outweighs the (100)-like character. It would be expected that (211)B orientation would be favored

for GaSb growth. However, growth on this orientation will tend to proceed in a (111)B-like fashion. In other words, growth on the (211)B should be considered as identical to growth on "tilted (111)B surface". It is expected that growth on (211)B face would confront the same difficulties as the (111)B surface, such as rough morphology, stacking faults, etc.. For the (511)B orientation and higher index planes, the (100)-like bond sites outnumber the (111)B-like bond sites and thus the (100)-like character will dominate. Growth on these orientations will adopt the (100) growth mode, but may not possess Sb rich enough environments. The (311)B surface, as shown in Fig. 2, consists of equal densities of single- and double-dangling bond sites resulting in equal weighting of the (111)B-like and (100)-like components. (311)B is the orientation which has the highest density of (111)B-like bond sites and still supports (100) growth mode since only a single-monolayer step exists and its terrace along (100) surface just consists of one atom, which is the shortest possible terrace width. Therefore, (311)B becomes the optimal choice for GaSb growth since it will support the step-terrace-kink growth mode and the surface structure is still 50% (111)B-like.

To study what we have presented above, GaSb/AlGaSb heterostructure MSM detector were prepared by MBE growth on semi-insulating InP substrates of (311)B and (100) orientations. The substrates of different orientations were mounted side by side for simultaneous growth of the MSM detector structure. The structure consisting of a 2 μm undoped $Al_{0.5}Ga_{0.5}Sb$ buffer layer followed by a 1.5 μm Te doped GaSb layer, 50 nm Te doped $Al_{0.5}Ga_{0.5}Sb$ barrier-enhancement layer, and 5 nm GaSb cap layer, which is also Te doped. The doping level of the samples were measured by Hall effect measurements at room temperature. The structure grown on (311)B shows n-type conductivity with a doping level of $1.5x10^{16}$ cm^{-3} and a mobility of 5500 $cm^2.V^{-1}.s^{-1}$, while the structure grown on (100) orientation exhibits p-type conductivity with a doping level of $8x10^{16}$ cm^{-3} and a mobility about 600 $cm^2.V^{-1}.s^{-1}$. The Schottky barrier

height between Al and the MBE grown strictures were measured by the standard I-V measurements. The Richardson plot of a Schottky contact on the (311)B sample is shown in Fig. 3. The barrier height of the (311)B sample is estimated about 0.6 eV, but the (100) sample showed ohmic behavior.

Interdigitated-finger structures with finger lengths and finger spacings from 1 to 4 μm and finger widths varying from 25 to 90 μm were fabricated using silicon nitride as a dielectric layer, aluminum as a metal barrier, and titanium-platinum-gold as the interconnect metal. At the a bias voltage of 2.5 V, the devices with an area of 25x25 μm^2 exhibit dark currents of ≈1 μA at 300 K and ≈0.1 nA at 77 K . Fig. 4 shows the results of the responsivity of the detectors as a function of incident optical power for various bias voltages, which were measured at 300 K. At low bias voltages, the responsivity is about 0.2 A/W; at high bias voltages, it exceeds 0.6 A/W which is close to the theoretical maximum. The intensity dependence of the responsivity is large at high bias voltages and is attributed to both the low frequency gain and the limitations on transport placed by an abrupt barrier. The use of graded junctions should decrease the latter effect. Fig. 5 shows the modulation response at room temperature for a large area detector at a wavelength of 1.3 μm. The 3 dB response bandwidth of the device exceed 1.0 GHz at a bias voltage of 2.5 V. The bandwidth is similar to those observed in similarly structured $Ga_{0.47}In_{0.53}As$ MSM detectors at similar bias voltages. Evidence regarding the hole velocities is inconclusive from these results.

In addition to room temperature characterization of the detector performance, we have also performed a similar measurement at 77K. A significant improvement in response was observed near 77 K as shown in Fig. 6. The laser excitation source used has a full-width-half-maximum (FWHM) of ≈ 23 ps and the photodetector shows

a response with a FWHM of ≈ 27 ps. This indicates an increase in hole mobility which leads to an improvement in the detector response in the initial part of the carrier collection process. The tail of this response corresponds to a velocity of 3×10^6 cm s^{-1} at an electric field of 2.5×10^3 Vcm^{-1}. The 3-dB bandwidth of the detector, based on these measurement, exceeds 10 GHz at the bias voltage of 5 V. This is a substantial improvement over $Ga_{0.47}In_{0.53}As$ MSM detectors which typically have 3-dB bandwidths of about 3-4 GHz under the same bias conditions. This low temperature response suggests an improvement in the characteristics of the detectors and can be attributed to the improvements in transport and storage of holes in these structures. The decrease in FWHM, largely associated with the peak response region and hence with high carrier densities in the detector, suggests both an improvement in the low-field velocity of carriers which occurs due to improvements in mobility, and the insignificant effect of collection inefficiencies at these large hole carrier densities. At 300 K, the mobilities in these structures are still low, similar to those of other III-V semiconductors, which is perhaps due to the effects of residual defects arising from the lattice-mismatched growth and residual impurities.

In conclusion, we have demonstrated the $Al_{0.5}Ga_{0.5}$/GaSb MSM detectors prepared on (311)B InP substrate. The results from Hall effect and I-V measurements have demonstrated that (311)B is the optimal choice for GaSb growth since it will support the step-terrace-kink growth mode and the surface structure is still 50% (111)B-like. The transient response of these devices is about 1 GHz at room temperature and exceeds 10 GHz at 77 K. This significant improvement is attributed to the improvements in hole transport and storage of holes in these structures. The less Sb-deficiency related p-type native defect density in the GaSb grown on (311)B

oriented substrates make this orientation the optimal choice for the fabrication of GaSb based electronic and photonic devices.

This work is supported by National Science Foundation with additional support from DARPA/NCIPT.

REFERENCES

1. D. L. Rogers, in Proc. LEOS' 90, Nov. 1990.

2. K. Kajiyama, Y. Mizushima, and S. Sakata, Appl. Phys. Lett.,**23**, 458, 1973.

3. J. Soole, H. Schumacher, H. P. Leblanc, R. Bhat, and M. A. Koza, IEEE Photon. Technol. Lett., **1**, 250, 1989.

4. C. X. Shi, D. Grutzmacher, M. Stollenwerk, Q. K. Wang, IEEE Trans. Electron Dev. **ED-39**, 1028, 1992

5. C. A. Mead and W. G. Spitzer, Phys. Rev. **134**, A713, 1964.

6. L. F. Luo, R. Bereford, W. I. Wang, and H. Munekata, Appl. Phys. Lett., **55**, 789, 1989.

7. L. F. Luo, K. F. Longenbach, and W. I. Wang, IEEE Electron Device Lett. **EDL-11**, 567, 1990

8. K. Yoh, T. Moriuchi, and Inoue, IEEE Electron Device Lett., **EDL-11**, 526, 1990.

9. D. Effer and P. J. Etter, J.Phys. Chem. Solids, **25**, 451, 1964

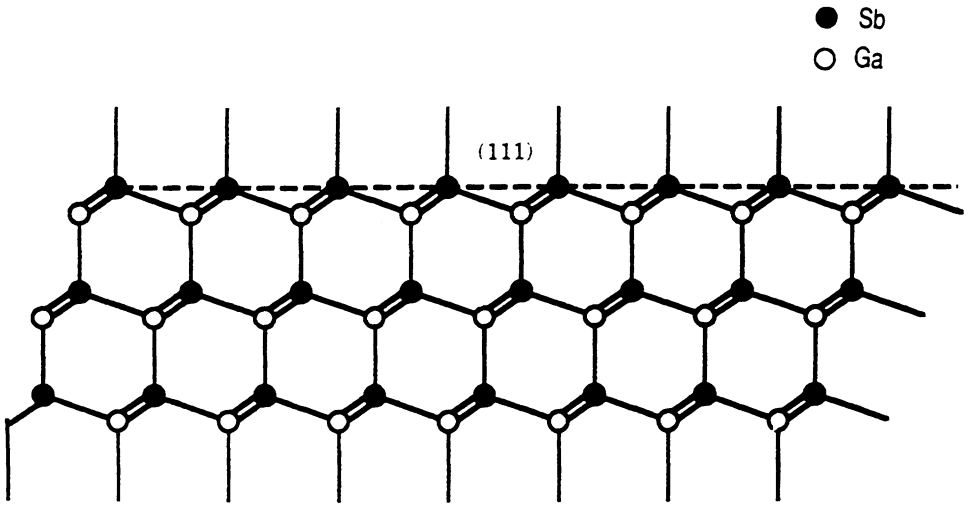

Fig. 1 (111)B GaSb viewed along the [0$\bar{1}$1] direction.

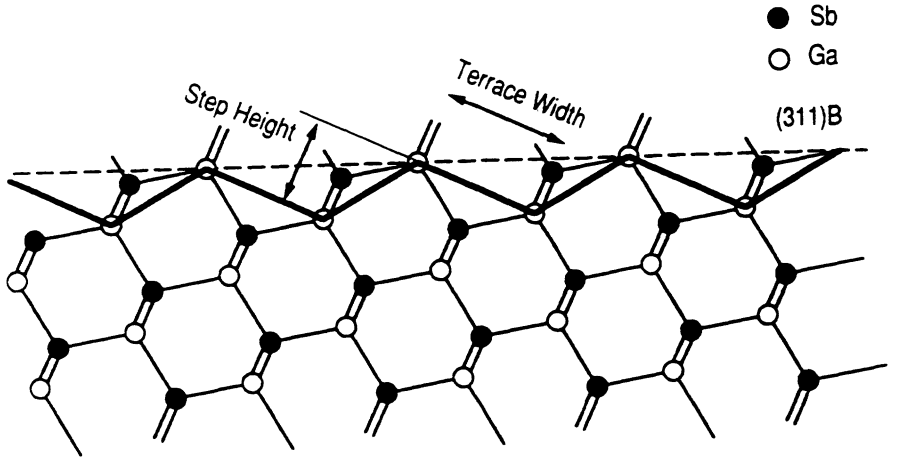

Fig. 2 (311)B GaSb viewed along the [0$\bar{1}$1] direction. The heavy line highlights the (100) terrace structure.

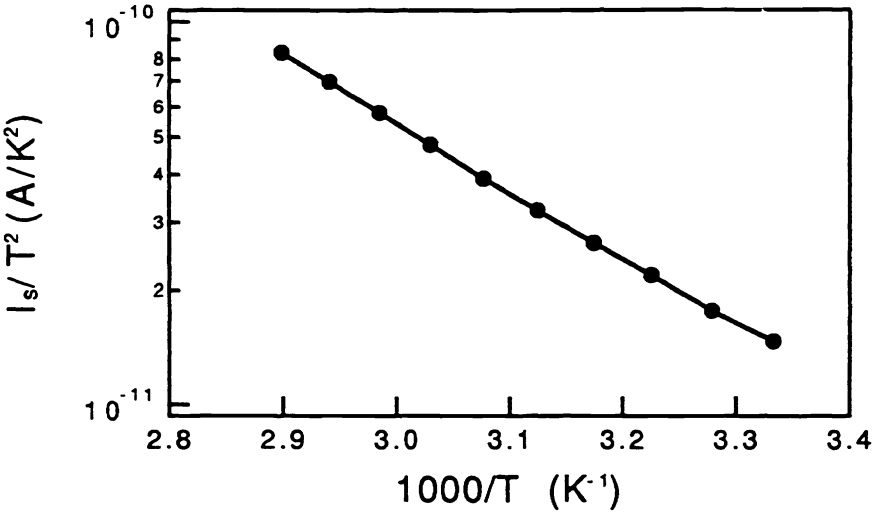

Fig. 3 The Richardson plot of a Schottky contact on the (311)B sample.

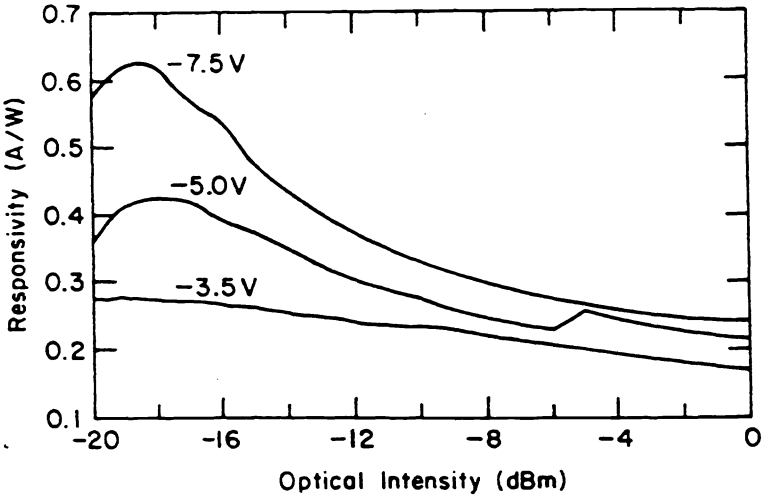

Fig. 4 Responsivity at 300 K as a function of optical intensity of 1.3 μm wavelength for various bias voltages. The responsivity varies between 0.18 and 0.63 A/W and is a function of optical intensity and applied bias.

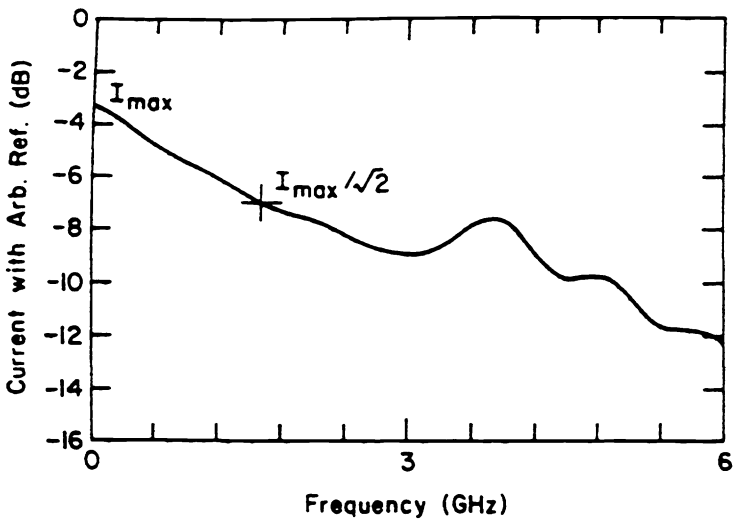

Fig. 5 The modulation response at 1.3 μm wavelength and 2.5 V bias voltage for a 90x90 μm^2 area MSM diode employing 2μm finger lengths and spacing.

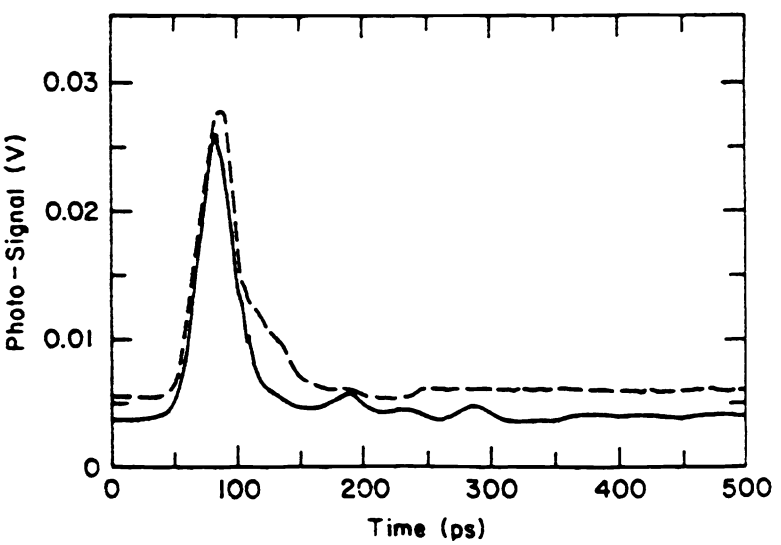

Fig. 6 The temporal response at 77 K to a laser pulse with FWHM of 23 ps. The solid line shows the detected laser signal, and the dashed line shows the detector signal. The bandwidth is estimated to estimated exceed 10 GHz.